Arab J Sci Eng (2014) 39:4165–4177
DOI 10.1007/s13369-014-1026-6

RESEARCH ARTICLE - MECHANICAL ENGINEERING

Numerical and Experimental Investigation of Plastic Interaction Between Rough Surfaces

Radosław Jedynak · Marian Sułek

Received: 28 February 2013 / Accepted: 15 April 2013 / Published online: 16 March 2014

Abstract The paper presents a dry friction model considering plastic interactions described by the Oxley equations. The model differs clearly from those published by Oxley due to the fact that it includes a statistical analysis of rough surface interactions. The contact of a single asperity is analyzed in a 3D—not 2D—space. The results of this analysis are further extended to the contact of two rough-surfaces by accomplishment of an appropriate summing (integration) of individual elementary forces of friction and pressure occurring in discreet contacts. In the case of papers based on the Oxley model, their authors analyze the contact of a single asperity with a plane and thus compute the macroscopic friction coefficient. On the basis of the achieved mathematical model of dry friction, the friction force was determined and consequently, the friction coefficient. In order to verify theoretical speculations, an experimental test was carried out in the system consisting of a steel disk with a galvanized coating and a steel pin. The results of experimental tests comply with the solutions achieved via a computer simulation. The resistance to motion results mainly from plastic deformations, which in turn result in adhesion tacking. Among investigated galvanic coatings, the highest motion resistance was revealed by a nickel coating, whereas the lowest one was revealed by a silver coating.

Keywords Asperity contact · Friction model · Plastic interaction

R. Jedynak (✉)
Kazimierz Pulaski University of Technology and Humanities,
Malczewskiego 29, 26-600 Radom, Poland
e-mail: jedynakr@pr.radom.pl

M. Sułek
Industrial Chemistry Research Institute,
Rydygiera 8, 01-793 Warsaw, Poland
e-mail: sulekmarian@wp.pl

الخلاصة

تقدم هذه الورقة العلمية نموذج الاحتكاك الجاف مع النظر في التفاعلات البلاستيكية التي وصفتها معادلات أوكسلي. وهذا النموذج يختلف بشكل واضح عن ذلك الذي نشرته أوكسلي، ويرجع ذلك إلى حقيقة أنه يتضمن تحليلا إحصائيا لتفاعلات السطح الخشن. وقد تم تحليل الاتصال من وجه منفرد في فضاء ثلاثي الأبعاد وليس ثنائي الأبعاد. وتم توسيع نتائج هذا التحليل إلى مزيد من الاتصال من اثنين من السطوح الخشنة عن طريق تحقيق جمع مناسب (التكامل) للقوى الابتدائية الفردية من الاحتكاك والضغط التي تحدث في اتصالات متحفظة. وفي حالة الأوراق العلمية المستندة إلى نموذج أوكسلي، فإن مؤلفيها يحللون الاتصال من الوجه المنفرد مع المستوى، وبالتالي حساب معامل الاحتكاك العياني.

وعلى أساس النموذج الرياضي المتحقق من الاحتكاك الجاف حُدّدت قوة الاحتكاك وكنتيجة لذلك حُدّدت معامل الاحتكاك. ومن أجل التحقق من التكهنات النظرية أجري اختبار تجريبي في نظام يتكون من قرص فولاذي مع طلاء مجلفن و دبوس فولاذي. ونتائج الاختبارات التجريبية تتطابق والحلول التي تحققت عن طريق المحاكاة الحاسوبية. ومقاومة الحركة تنتج أساسا من التشوهات البلاستيكية التي تؤدي بدورها في تغير اتجاه الالتصاق. ومن بين الطلاءات المجلفنة التي حُقّق فيها، تم الكشف عن أعلى مقاومة حركة من قبل طلاء النيكل في حين تم الكشف أن طلاء الفضة هو الأدنى.

List of symbols

a	Radius of the area of contact
A'	Area of a single plastic contact
A_n	Nominal contact area
A_r	Real contact area
b, ν	Parameters of bearing surface curve
c	Approach of the mating surfaces for bearing surface curve (measured fromthe highest asperity)
d	Mutual overlapping of maximum asperities
f	Relative strength of connections
h	Mutual overlapping of two given asperities
k	Shear strength of the deformed material (shear yield stress)
m	Linear density of profile heights (number of peaks per 1mm of theprofile)

n	Density of asperities of contacting areas
N	Normal force
N_R	Number of profile peaks over the 10 mm section
p	Pressure
P	Elementary force between two asperities
P_z	Elementary normal force (normal force on a single asperity)
P_x	Elementary friction force (friction force on a single asperity)
r	Parameter of mutual asperity overlapping
r_{max}	Border parameter of asperity penetration
R	Radius of hemispherical asperity
R_a	Arithmetic mean deviations of roughness profile
R_{max}	Maximum roughness height
R_q	Quadratic mean deviations of roughness profile
R_t	Sum of the curvature radii of contacting asperities
S	Standard deviation of asperity heights
S_m	Mean spacing of profile irregularities
T	Friction force
t_p	Bearing ratio (relative reference length of profile)
z	Height of asperity measured from the mean of asperity heights
δ	Separation distance of asperities along the normal to the contactpoint
ε	Relative approach for bearing surface curve
$\phi(z)$	Distribution function of asperity heights
τ	Shear strength of the interfacial film
μ	Coefficient of friction

1 Introduction

The user expects maximum efficiency, reliability and durability of the machinery and equipment he uses accompanied by the highest economical benefits (minimum costs). Movable friction pairs play a crucial role in meeting these requirements. The processes occurring in them are responsible for energy losses and wear of contacting elements. One of the most important tasks in the field of machine performance and reliability is the possibility of theoretical assessment of the resistance to motion of the contacting friction planes. It is important in the areas where dry friction occurs especially when its high value can lead to the excessive wear of contacting planes, generation of too much heat which can entail seizures. Minimizing the resistance to motion leads to energy saving, reduced wear and longer usage. On the other hand, increased ability to counteract seizure reduces the possibilities of device failure. Favourable tribological properties can be obtained through the appropriate selection of materials and formation of a surface topography.

Modelling of the contact between moving rough surfaces allows a better understanding of friction and wear mechanisms, which can be used in engineering solutions. This issue has been examined using a number of approaches. The statistical type of a contact model is still the most popular model used in rough surfaces contact. Instead of using the complete roughness data, only probability density function is used. This function means the probability of the asperity with the height between h and $h + \mathrm{d}h$.

The first well known statistical model was introduced by Greenwood and Williamson [1] (GW). They joined a statistical process with a classical Hertzian contact to deal with the rough surfaces contact. They adopted the following assumptions: (1) the asperity height distribution is Gaussian, (2) asperity contact is modelled by the Hertzian spherical contact theory, (3) the asperity tip radius is assumed constant and (4) ignore adhesion, neighbouring asperity interaction and shoulder–shoulder contact. A rough surface was described by three parameters: (1) standard deviation of asperity height distribution, (2) average asperity summit radius of curvature and (3) areal asperity density.

This model has been widely accepted and developed by numerous researchers. The main reason of its popularity is its simplicity and predictions are in accordance with the carried out experiments. Adams and Nosonovsky [2] summarized various modifications of the GW model in their review paper. Other interesting review articles are written by Bhushan [3], Liu [4], Barber [5], Buczkowski and Kleiber [6]. To summarize these trends we can say: proposed models take into account different aspects of surface topography, the effects of friction, plasticity, adhesion and more complex local surface topography.

The GW model has been modified a number of times by other researchers. More significant modifications are briefly reported below.

The model proposed by Greenwood and Tripp [7] extended the GW model to contact between two rough surfaces. Greenwood and Tripp (GT) showed that the contact between two rough surfaces can be modelled by a contact between an equivalent single rough surface and a flat. The equivalent rough surface is characterized by an asperity curvature and the peak-height distribution of the equivalent surface. They gave the simple formula for a standard deviation of the statistical distribution.

There are a few approximation formulas for the integrals given by the GT model. Recently Jedynak and Gilewicz [8] proposed a new formula which is based on the Pade theory. This approximation method has become increasingly popular for solving different problems in mechanics. They compared the approximation formula with others. The results show that their formula is more accurate than the currently used one.

Whitehouse and Archard [9] extended the GW model by abandoning the assumption of a constant asperity radius. They found from a profilometer study of rough surfaces that higher asperities have sharper tips. On the basis of this fact they derived the joint probability density function of both summit height and summit curvature.

Nayak [10] introduced the techniques of random process theory into the analysis of Gaussian rough surfaces. He considered a more complex statistical model which characterizes a random surface by three spectral moments of the profile, which are equivalent to the variances of the distribution of profile heights, slopes and curvature respectively.

Tsukizoe and Hisakado [11] assumed a conical shape for surface asperities. They proposed a statistical contact model for predicting the contact spot size and density for an isotropic Gaussian rough surface in contact with an ideal smooth flat surface.

Bush et al. [12] (BGT) extended the Nayak statistical model by considering elastic contact model which treated asperities as elliptical paraboloids with two principle curvatures of asperities along the x and y directions. The BGT model became more generalized Hertzian elliptic contact model. In another paper Bush et al. [13] considered a rough surface with a random anisotropic distribution of asperity radii.

McCool [14] derived the closed-form expressions of areal asperity density, average asperity summit radius of curvature and standard deviation of asperity height distribution for the GW model based on the Nayak statistical model for isotropic rough surfaces. In another paper McCool [15] extended the GW microcontact model to include skewness in the distribution of surface summit heights and the presence of a surface coating of prescribed thickness.

Chang et al. [16] proposed a method for treating elastic–plastic contact of rough surfaces. This model is widely known as the CEB model. This CEB model assumes that the hemisphere deformation is localized near its tip, the hemisphere behaves elastically below the critical interference and fully plastically above that value and the volume of the plastically deformed hemisphere is conserved.

Zhao et al. [17] extended an elasto-plastic asperity contact model for rough surfaces (ZMC). They considered three regions of (1) fully elastic, (2) elastic–plastic and (3) fully plastic contacts. The relations for contact area, contact load for the elastic region are similar to those of the CEB model. They introduced a "template" cubic polynomial function which satisfies continuity of the function and smooth transition between mentioned segments.

Persson [18] reviewed basic contact mechanics theories for surfaces with random roughness. He briefly discussed the Hertz contact theory for elastic spheres with perfectly smooth surfaces and then the GW and BGT models. In most cases the elastic coupling between the asperity contact regions is neglected. His theory breaks this limit and is valid for all squeezing (normal) forces.

A fractal description of engineering surfaces is another method used in the contact mechanics. This method is presently a subject of the intensive discussion. The surface roughness can be described using two scale-independent parameters D and G, where D relates to distributions of different frequencies in the surface profile and G to the magnitude of variations at all frequencies. Majumdar and Bhushan [19] developed the first elastic multi-scale contact model based on fractal geometry. They assumed a Gaussian distribution of heights and deduced the formula of contact load as a function of geometrically-dependent parameters D and G and the elastic properties. The present fractal contact theory suffers from a few serious problems like (1) the distribution of contact areas is assumed geometrically and does not take into account the actual elasticity (2) it predicts that the lighter the load, the greater will be the percentage of contacts that are plastically deformed. Other fractal-based models have also been developed by a number of investigators.

Jackson and Streator [20] (JS) developed an isotropic 3D multi-scale contact model based on 3D sinusoidal contact model. The main idea of the JS model is that a 2D rough surface profile can be decomposed into stacks of sinusoidal waves with different frequencies and amplitude. In the following paper Jackson [21] simplified solution of the full multiscale model which was presented by JS to the stacked multiscale model. Ciavarella et al. [22] suggested a new "discrete" GW model, which takes input data directly from numerical discretizations of surfaces. They developed a full interaction asperity algorithm. The results obtained with this model and using fractal surfaces show that the original GW theory correctly or at least qualitatively predicts the basic features of the problem. In another work Ciavarella et al. [23] formulated an improved version of the GW theory with the inclusion of interaction between asperities. They claimed that improved GW theory is able to predict the numerically obtained contact response for intermediate load levels. Numerical contact simulations using Weierstrass–Mandelbrot surfaces show a general agreement with the improved theory.

This method is rather controversial between researchers, for example Whitehouse [24] questioned the philosophy of using fractals to describe and control engineering surfaces. Greenwood [25] in his comments on the paper of Whitehouse agreed with him and stated that fractals have been "overhyped".

Another approach is connected with using of the finite element method (FEM) to study the elastic–plastic contact of a contact between single asperity and flat surface. One of the most popular work on this subject is paper written by Kogut and Etsion [26] (KE). They presented an elastic–plastic finite element model for the frictionless contact of a deformable sphere pressed by a rigid flat. They analyzed evolution of the elastic–plastic contact with increasing interference. The model shows three distinct stages of deformation that range from fully elastic through elastic–plastic to fully plastic contact interface. It offered a general dimensionless relation for the contact load, contact area and mean contact pressure as a function of contact interferences. Jackson et al. [27] analyzed

sliding interaction between spheres using two approaches: a semi-analytical and finite element simulation. These analyzes were used to formulate empirical equations, which describe the average tangential and normal forces resulting from the sliding interaction. The study showed that the effective friction coefficient between spherical asperities increases with the elastic modulus, decreases with yield strength, and increases with the interference between the contacts.

Malayamurthi and Marappan [28] presented a contact analysis between a deformable sphere and a rigid flat by a finite element method. They carried out the analysis beyond elastic limit for various materials with different radii. Thanks to these studies they found some materials which showed vitally different contact phenomena.

Shankar and Mayuram [29] developed a finite element method to calculate the wear depth and volume of material displaced laterally between two contacting asperities during a sliding. They were able to predict the wear by combining the influences of contact stress and a surface wear coefficient. They claim that understanding the nature of the sliding interactions between two contacting asperities allows a better insight into the wear as well as frictional process.

Vijaywargiya and Green [30] presented the results of a finite element analysis used to simulate a two-dimensional (2D) sliding between two interfering elasto-plastic cylinders. The results were presented for both frictionless and frictional sliding. Mulvihill et al. [31] introduced a finite-element model of the interaction of an elastic–plastic asperity junction based on cylindrical or spherical asperities. The model was used to predict sliding friction coefficients. It differs from the previous work by permitting greater asperity overlaps, enforcing an interface adhesional shear strength, and allowing material failure.

The FEM was also used to construct models of multi-asperity contacts. In another work Kogut and Etsion [32] presented an improved elastic–plastic model for the contact of rough surfaces. This model is based on an accurate finite-element model solution of a single asperity contact. It predicts the contact parameters such as a real area of contact, a real contact pressure as function of contact load and others. The model proposed by Cohen et al. [33] also incorporates an accurate finite element analysis for contact and sliding inception of a single elastic–plastic asperity in a statistical representation of surface roughness. A comparison between the present model and a previously published friction model shows that the latter severely underestimates the maximum friction force by up to three orders of magnitude.

Abdo [34] also presented an improved mathematical elastic–plastic model for the contact of rough surfaces. It is based on an accurate finite element solution of a deformable single asperity and a rigid flat surface. This model provides dimensionless expressions for the contact area and contact load. It differs from the existing models because it takes into account the level of interference beyond expected failure. This model considers a realistic picture of elastic–plastic deformation where elastic, plastic and failure behaviours can occur simultaneously for an asperity.

Recently Jackson and Green [35] compared the four contact models: (1) GW (with a Gaussian distribution) [1], (2) BGT statistical model [12], (3) Persson's diffusion model [18] and (4) Jackson's stacked multiscale model [21] to a deterministic elastic contact model that uses a fast Fourier transform. The deterministic model is considered as the most accurate because surfaces are analyzed from actual measurements and then can be used for modelling parameters of contact. The results for different surfaces show that four mentioned models produce nearly linear predictions of contact area as a function of load and in some cases are even in quantitative agreement. Jackson and Green state that these four models cannot make exact quantitative predictions of rough surface contact because they use only a few key parameters from the complex surface profile.

The analysis of surface topography is a subject which is still being developed by many researchers. It is difficult to describe rough surface deterministically due to its multi-scale structure and random nature. Therefore, statistical parameters of rough surfaces are used. Research in this area is extensive. We would like to pay attention to two papers: Pawar et al. [36] and Robbe-Valloire [37]. Recently Pawar et al. found that the contact parameters vary significantly based on the method used to determine the topography parameters, and as a function of the autocorrelation length of the surface, as well as the sampling interval. They claim that using a summit identification model or the GW model based on topography parameters obtained from a summit identification scheme is the most reliable approach. The summit identification method is the method which finds the surface topography parameters. It is based on determining the summits of the surface as local maxima using an 8-nearest neighbour summit identification scheme.

Statistical analysis of asperities on a rough surface made by Robbe-Valloire [37] delivered a lot of useful relationships between roughness parameters measured by typical profilometer and surface topography characteristics like: areal density of asperity, the mean radius of the asperities and others. These relationships were very helpful in experimental part of this paper to calculate surface statistics from profile data which were needed in computer simulation of coefficient of friction.

Recently Kapłonek and Nadolny [38] showed useful analysis of a possible use of laser scatterometry and image processing in the optical inspection of the condition of the examined surface topography.

At this point it is worth noting the studies which were made by Abdo [39]. He joined results of surface topography examinations with friction experiments. He considered the mechan-

ical interaction due to surface roughness and examined the surface theories using the classical definition of coefficient of friction. He carried out experiments with pin-on-disk test apparatus. In each case, he performed profilometer measurements on the disks and determined the Greenwood and Williamson parameters. Next he compared theoretical values of friction coefficients with those obtained from measurements for various applied normal loads. The results suggested that the elastic–plastic formulations provide better predictions of load ratios than the elastic contact formulations.

To summarize this review of different models it can be said that there is still a lack of spatial contact models. Such models take into account a shoulder–shoulder contact of asperities that results in a slanted orientation of forces due to a contact slope. These contact forces consist of both parallel and perpendicular components to mean plane. Sepehri and Farhang model [40] is one of a few works which extended a finite element model of the elastic–plastic interaction proposed by Kogut and Etsion [26] to a 3D contact of two nominally flat rough surfaces.

Another interesting approach is proposed by Karpenko and Akay [41]. They derived a computational method for the calculation of the friction force between 3D rough surfaces. They assumed the friction force to come from the elastic asperity deformation and the shear resistance of adhesive junctions at the contact areas. They computed contact force distribution using an iterative procedure which considered contact parameters, external loads and surface topographies. The process of iteration was carried out until the sum of normal components of contact forces equalled the normal load. They proved that by increasing surface roughness a value coefficient of friction decreases exponentially.

In this paper, we consider plastic contact of nominally flat rough surfaces. It is a new spatial contact model which is based on the slip-line theory for plastic deformation. The contact model described in the next section considers two rough surfaces sliding along a straight line parallel to the mean planes of the surfaces. The surfaces come into contact under the action of an external normal load, P. The contact model considers the contributions of forces developed at each asperity contact resulting from their plastic deformation and shear resistance due to adhesion. This model can be easily extended to elastic–plastic one. If we would like to extend this model to elastic–plastic one we should introduce the parameter of critical asperity deformation for an elastic contact. If we assume that all asperities whose deformations are larger than the critical interference have plastic deformation and below elastic deformation we can sum all elementary forces for plastic and elastic asperities interactions and thus calculate normal and tangential forces. In this case the elastic deformation is defined by Hertzian spherical contact theory. Preliminary calculations performed for the elastic–plastic model and for information received from the experiment showed that we can neglect the effect of elastic interactions for macroscopic forces and that is why we present a model only for plastic deformation. This statement is true for range of loads used in the experiment and state of surface roughness. Our earlier model for elastic contact of two rough surfaces was presented in the publications of a limited circulation.

2 Basic Assumptions of the Model of Plastic Interactions

Analysis of the contact of two rough surfaces was started with the construction of a model of interactions between two single asperities. The starting point for this model was Shcheglovov's geometry [42]. For the sake of the model it was assumed that the contact between rough surfaces is of a discreet nature, i.e. it occurs between two single asperities. Next, on the basis of the said geometrical model, using the statistics of asperity distribution and the type of interactions between them, the forces of pressure, friction and the friction coefficient were determined.

The contact of two single asperities (Fig. 1) is described by the following parameters:

h—mutual overlapping of two considered asperities (along the normal to the plane of motion),

$\delta = R_t - \sqrt{(R_t - h)^2 + r^2}$—a separation distance of an asperity along the normal to the contact point, ($R_t = R_1 + R_2$—the sum of the curvature radii of the contacting asperities),

r—parameter of the asperity overlaps (for $r = 0$ contact of the peaks).

The model assumes that the contact between rough surfaces is discreet in nature, i.e. it occurs between single asperities.

In Fig. 1 the following forces occurring in the contact between two asperities are marked: P_z elementary pressure and P_x elementary friction. On the basis of the geometrical model and with the use of the asperity distribution statistic and the type of interactions between asperities, the total pressure N (Eq. 1) and total friction T (Eq. 3) which operate between rough surfaces were calculated as well as friction coefficient μ (Eq. 5). These forces were determined by summing the elementary forces in all asperity contacts.

For the sake of the plastic interaction analysis the model put forward by Oxley [43] for the elementary asperity contact was adopted as the starting point. The following assumptions were adopted while solving the problem: deformation occurs in the flat 2D deformation without flowing of the material in the direction normal to the relative motion of the asperity, the deforming material is ideally rigid-plastic, it is isotropic due to the deformation direction and its density is constant. The phenomenon of plastic hardening is not taken into account.

The solution put forward by Oxley [43] describes the situation of a surface contact between objects of moderate rough-

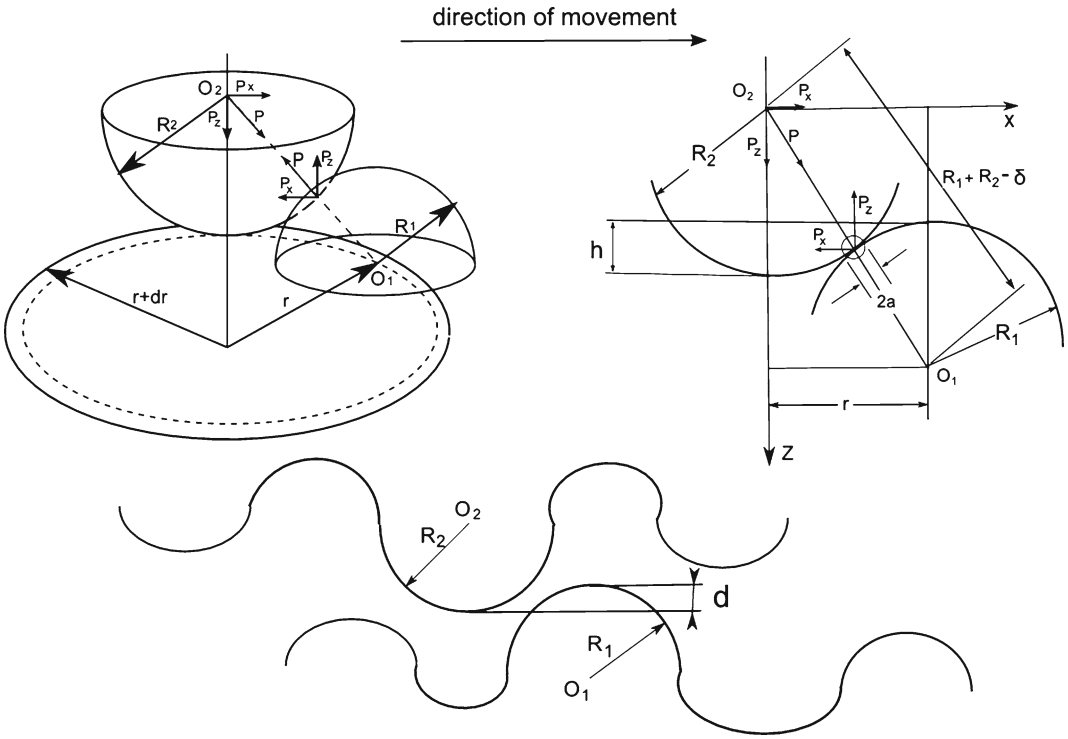

Fig. 1 Stereometric contact of two asperities in the proposed theoretical model

ness, characterized also by small adhesion. Consequently this means low friction coefficients. The wear process is connected with the occurrence of a buildup of deformed material in the form of a relocating wave in front of the asperities of the rigid body. The choice of this model for the description of elementary plastic interactions was favoured, among others, on account of a large number of references to it in tribological literature [44,45], as well as its high compatibility with experimental results which verify its correctness. As a curiosity it can be mentioned that Jahanandish et al. [46] used slip-line theory in geotechnical engineering practices. They obtained the new bearing capacity formula from the solution of the plasticity equations based on soil rupture mechanisms similar to those suggested by Oxley for penetration of punches into metal.

The works using the formulas given by Oxley always use analysis of a single asperity with a plane [43,44]. In the proposed model the values of pressure and friction were calculated with the use of the statistical distribution of asperity heights covering two rough surfaces and the plastic nature of their interactions. Such an approach is different from that described by Oxley.

2.1 Normal force (N) in a plastic contact

The elementary normal force P_z appearing in contact of two asperities was determined from the slip-line field [43]. While determining the total force N, the statistical approach was used which was not applied in the Oxley model [43]. The function of the asperity height distribution $\phi(z)$ was introduced. In this way a formula in the form of the triple parametric integral was obtained, where parameter d describes mutual overlapping of maximum asperities:

$$N = \pi A_n n_1 n_2 \int_0^d \int_0^{d-z_1} \int_0^{r_{\max}} P_z \phi(z_1)\phi(z_2) r \mathrm{d}r \mathrm{d}z_2 \mathrm{d}z_1, \qquad (1)$$

where: A_n, the nominal contact area,

n_i, density of asperities of contacting areas,

$P_z = k\left\{\left[1 + 2(\frac{\pi}{4} + \phi - \eta)\right]\cos\alpha + \sin(\alpha + 2\phi)\right\} A'$ elementary pressure (Fig. 1),

$A' = \pi \frac{R_1 R_2}{R_1 + R_2}\delta$, area of a single plastic contact [18],

$\phi(z)$, statistical distribution of asperity heights,

$r_{\max} = \sqrt{2R_t h - h^2}$, border parameter of asperity penetration,

$$\sin\alpha = \frac{r}{R_t - \delta},\ \alpha + \phi = \frac{1}{2}\arccos f,\ \sin\eta = \frac{\sin\alpha}{\sqrt{1-f}},$$

h, mutual overlapping of two considered asperities (along the normal to the plane of motion),

$\delta = R_t - \sqrt{(R_t - h)^2 + r^2}$, separation distance of asperities along the normal to the contact point,

$R_t = R_1 + R_2$, sum of the curvature radii of contacting asperities,

r, parameter of mutual asperity overlapping,

$f = \frac{\tau}{k}$, "relative strength of connections" [43] defined as the ratio of the shear strength of the interfacial film τ and k—shear strength (shear yield stress) of the softer workpiece material.

Physical interpretation of the triple parametric integral in formula (1) without P_z is the number of asperity contacts. For numerical calculations, formula (1) describing normal force was converted with the use of geometrical dependencies following formula (1). What is more, the integration variable r was replaced by the angular α:

$$N = \pi^2 A_n n_1 n_2 k R_r \int_0^d \int_0^{d-z_1} \int_0^{\alpha_{\max}} V(\alpha, z_1, z_2)\phi(z_1) \times \phi(z_2)\mathrm{d}\alpha\mathrm{d}z_2\mathrm{d}z_1 \quad (2)$$

where:

$$V(\alpha, z_1, z_2) = \frac{(R_t - h)^2 \sin\alpha}{\cos^2\alpha}[Z(\alpha) - f\tan\alpha] \times [R_t(\cos\alpha - 1) + h]$$

$$\alpha_{\max} = \operatorname{arctg}\frac{r_{\max}}{R_t - h} = \operatorname{arctg}\frac{\sqrt{2R_t h - h^2}}{R_t - h},$$

$$\lambda = 1 + \frac{\pi}{2} + \arccos f + \sqrt{1 - f^2}.$$

Normal force N was determined numerically on the basis of formula (2).

2.2 Friction Force (T) in a Plastic Contact

Elementary friction force P_x occurring in contact of two asperities was also determined from the slip-line field [43]. In this case, the friction force T can be presented in the form of the triple integral:

$$T = \pi A_n n_1 n_2 \int_0^d \int_0^{d-z_1} \int_0^{r_{\max}} P_x \phi(z_1)\,\phi(z_2) r\mathrm{d}r\mathrm{d}z_2\mathrm{d}z_1, \quad (3)$$

where: $P_x = k\left\{\left[1 + 2(\frac{\pi}{4} + \phi - \eta)\right]\sin\alpha + \cos(\alpha + 2\phi)\right\}$ A′—is an elementary friction force.

For the sake of numerical calculations, formula (3) describing the friction force T was transformed with the use of geometrical dependencies following formula (1). What is more, the integration variable r was replaced by the angular α:

$$T = \pi^2 A_n n_1 n_2 k R_r \int_0^d \int_0^{d-z_1} \int_0^{\alpha_{\max}} \mathrm{U}(\alpha, z_1, z_2) \times \phi(z_1)\,\phi(z_2)\mathrm{d}\alpha\mathrm{d}z_2\mathrm{d}z_1 \quad (4)$$

where:

$$U(\alpha, z_1, z_2) = \frac{(R_t - h)^2 \sin\alpha}{\cos^2\alpha}[Z(\alpha) - f\tan\alpha] \times [R_t(\cos\alpha - 1) + h]$$

$$Z(\alpha) = \lambda - 2\alpha - 2\arcsin\left(\frac{\sin\alpha}{\sqrt{1 - f}}\right)$$

Friction was determined numerically on the basis of formula (4).

2.3 Friction Coefficient (μ) in a Plastic Contact

On the basis of the determined values of the friction force T and normal force N, the average coefficient of friction was calculated as the ratio of these values: $\mu = \frac{T}{N}$.

Substituting appropriate values (Eqs. 2 and 4) for T and N, we obtain:

$$\mu = \frac{\int_0^d \int_0^{d-z_1} \int_0^{r_{\max}} \left\{\left[1 + 2(\frac{\pi}{4} + \phi - \eta)\right]\sin\alpha + \cos(\alpha + 2\phi)\right\} \delta\phi(z_1)\phi(z_2) r\mathrm{d}r\mathrm{d}z_2\mathrm{d}z_1}{\int_0^d \int_0^{d-z_1} \int_0^{r_{\max}} \left\{\left[1 + 2(\frac{\pi}{4} + \phi - \eta)\right]\cos\alpha + \sin(\alpha + 2\phi)\right\} \delta\phi(z_1)\phi(z_2) r\mathrm{d}r\mathrm{d}z_2\mathrm{d}z_1}. \quad (5)$$

Later, the obtained Eqs. (2, 4, 5) will allow us to determine the values of normal force, friction force and friction coefficient for the given geometry and material constants characterizing the friction pairs.

3 Computer Simulation of Friction Coefficient

This section analyzes the results of computer modeling. The purpose of this analysis is computing the friction coefficient and comparing the values obtained with those achieved experimentally. In the experiment we used the disks covered galvanically with different metals. Each coating had about 20 μm thickness. We chose a very short initial time (120 s) for measurement of the coefficient of friction which guaranteed the stability of each coating. We assumed that such disks can be treated as homogeneous with known topography measured before the experiment.

3.1 Analysis of Surface Roughness

As the formerly described theoretical model of external friction is closely connected with the geometrical structure of

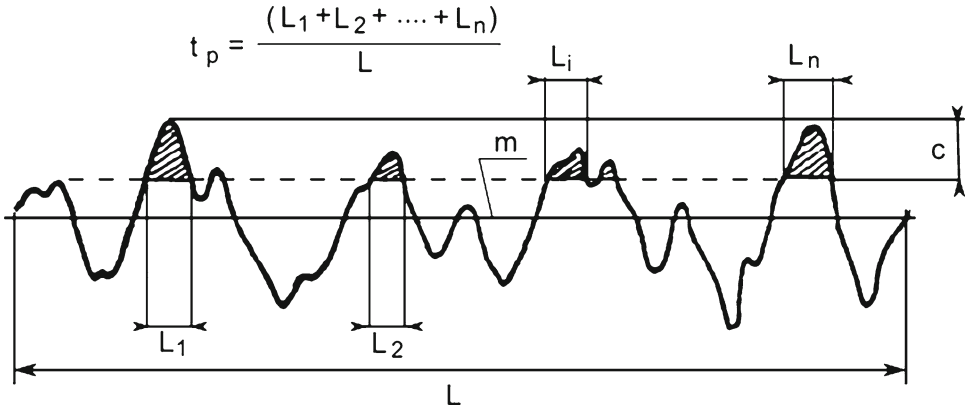

Fig. 2 Diagram for calculating bearing ratio t_p (c—approach of the mating surfaces measured from the highest asperity, m—mean of surface heights, L_i—individual length of the peak section at the level c)

Table 1 Material constants and parameters used for computer simulation in the experimental part of the work dealing with coatings

Material	Microhardness (MPa)	Maximum asperity heights R_{max} (μm)	Average curvature radii R (μm)	Density of asperity peaks per mm^2
Steel 45 (pin)	2,350	$R_{max} = 3.0 \pm 0.4$	$R = 79 \pm 7$	$n = 660 \pm 40$
Ag (disk)	700	$R_{max} = 1.4 \pm 0.3$	$R = 480 \pm 80$	$n = 180 \pm 40$
Cr (disk)	10,000	$R_{max} = 7 \pm 2$	$R = 46 \pm 6$	$n = 880 \pm 80$
Cu (disk)	700	$R_{max} = 5 \pm 2$	$R = 530 \pm 80$	$n = 50 \pm 20$
Ni (disk)	1,500	$R_{max} = 1.7 \pm 0.6$	$R = 450 \pm 60$	$n = 150 \pm 30$
Zn(disk)	600	$R_{max} = 2.5 \pm 0.5$	$R = 400 \pm 60$	$n = 180 \pm 40$
Steel 45 (disk prior to galvanic coating)	2,350	$R_{max} = 2.7 \pm 0.2$	$R = 50 \pm 5$	$n = 2{,}000 \pm 100$

contacting surfaces (their roughness), it seemed justified to examine the roughness of the samples prepared for the friction experiment. Surface roughness of the tested elements was determined by means of the Hommel T-2000 surface profile tester. Three measurements were taken for each working surface of the sample, perpendicular to the direction of the machining traces, in three places chosen at random, but in the vicinity of the predicted friction traces. Sample measurement results were averaged. The samples having similar characteristics (the same roughness class) were chosen for further friction tests. The report on measurements included the following parameters:

- arithmetic mean deviations of roughness profile (R_a),
- quadratic mean deviations of roughness profile (R_q),
- maximum roughness height (R_{max}),
- average roughness separation distance (S_m),
- number of profile peaks over the 10 mm section (N_r),
- and graphs of the profile and bearing ratio t_p (Fig. 2).

Bearing ratio t_p is the length of a bearing surface expressed as a fraction (or percentage) of the assessment length L at a depth c, or "slice level", below the highest peak. Mathematically it can be expressed

$$t_p = \frac{\sum_{i=1}^{n} L_i}{L}$$

In order to calculate the density of asperities (n), the formula given by Robbe-Valloire [37] for the isotropic surface was applied:

$$n = 1.2\,\mathrm{m}^2 \ (\mathrm{mm}^{-2})$$

where: m denotes linear density of profile heights (number of peaks per 1 mm of the profile).

The report on experiments gives the magnitude N_r, which indicates the number of the profile peaks over the length of 10 mm. Thus, we can assume that:

$$n = 1.2\left(\frac{N_r}{10}\right)^2 \ (\mathrm{mm}^{-2})$$

The radius of the asperity curvature (R) was determined by means of an empirical formula given by Whitehouse [47]:

$$R = 0.05\frac{S_m^2}{R_a} \ (\mu\mathrm{m})$$

R_{max} was adopted as the maximum asperity height directly from the report on experiments. The bearing curve obtained in the said profilometric examinations was used for the assessment of the distribution of asperity heights.

The magnitudes describing the topography of the sample surfaces calculated on the basis of the quoted statistical formulas taken from literature are presented in Table 1. The Table also includes mean values of microhardness of the examined galvanic coatings.

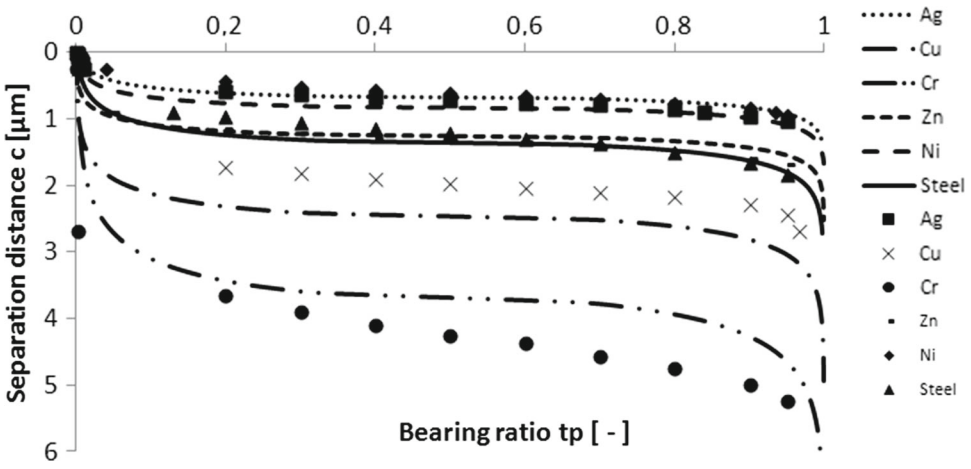

Fig. 3 Theoretical bearing ratio calculated from normal distribution (*continuous line*) for disks covered with different coatings and a steel disk. *Points* denote reported empirical results for the determined bearing curves

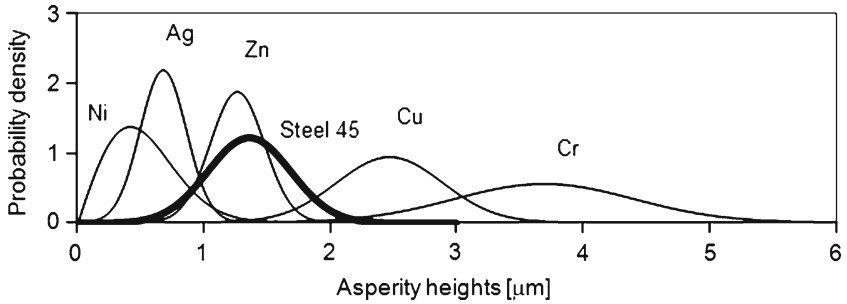

Fig. 4 Distributions of probability density of asperity heights for different galvanic coatings. The *thick line* indicates the distribution for the disk prior to coating (steel 45)

3.2 Results and Discussion of Results of Research Into Rough Surfaces

Figure 3 presents results of theoretical analysis of bearing area distributions for the examined disks. The continuous line denotes the Gaussian cumulative distribution function. The points denote empirical results reported for the bearing curve. In the case of all disks the distribution of asperity heights can be well described by means of the normal distribution. This results from a good compatibility of experimental bearing distributions and the appropriate Gaussian cumulative distribution functions. Table 1 contains results of asperity distribution analysis for particular coatings.

Obtained results for heights of the highest asperities, average curvature radii and surface densities of asperity peaks for particular galvanic coatings (Table 1) are worth comparing with appropriate steel disk parameters. While comparing asperity curvature radii of the disk before and after coating we can notice that in most cases they increase. The maximum increase of the radius is observed in the case of copper (11-fold). An exception is the chromium coating in the case of which we can notice a small decrease in this value (8 %). In the case of surface density of asperities we always observe its decrease following the coating process. Copper is characterized by the least number of asperities per a unit area. When it comes to an asperity height distribution (Fig. 4) we can say that galvanic coating modifies its form (it affects the value of standard deviation and the mean value). Both reduced (silver, zinc) and increased (copper and chromium) standard deviations are observed. The maximum decline in standard deviation was observed for a silver coating (45 %), whereas the maximum increase was noted for a chromium coating (115 %). Thus, in the case of silver and zinc coatings asperity heights are more concentrated around the mean value than prior to coating whereas in the case of copper and chromium coats a much broader distribution of asperity heights is obtained ("more broadening" around the mean value) in comparison to the initial situation (Fig. 4). Bibliographical item [48] outlines research results for coatings of zinc and chromium. Only one parameter characterizing surface roughness is analyzed, namely the arithmetic mean deviations of the roughness profile (R_a). Qualitative results are close to those presented in this paper. Another paper [49] presents results from tribological tests which were performed with electroplated copper and zinc coatings. Authors tried to explain wear mechanisms which took place during these tests. The performed Roentgen tests showed that copper (or zinc) transferred from the disc to the pin as the result of friction. On the basis of changes in topography of surfaces they concluded that in the case of copper adhesive wear was dominant, while for zinc–abrasive.

We can also investigate the effect of the type of the galvanic coating applied on the bearing capacity of examined disks. On the basis of the experimental results for the bearing

Table 2 Parameters of the bearing curve determined by the method of least squares for the tested surfaces with galvanic coatings, the steel pin contacting them and the steel disk prior to galvanic coating

Coating	$b\,(-)$	$\nu\,(-)$	$\varepsilon = \frac{c}{R_{\max}}(\%)$	$t_p = b\epsilon^{\nu}(\%)$
Cr	0.1 ± 0.2	1 ± 1	20	1 ± 3
Zn	1.8 ± 0.6	2.8 ± 0.2	20	2 ± 1
Ag	0.6 ± 0.3	1.7 ± 0.2	20	4 ± 2
Ni	11 ± 2	3.17 ± 0.08	20	7 ± 1
Cu	4.0 ± 0.6	2.29 ± 0.08	20	10 ± 2
Steel 45 (disk prior to coating)	14 ± 3	4.2 ± 0.2	20	2 ± 1
Steel 45 (pin)	4.1 ± 0.6	2.47 ± 0.07	20	8 ± 2

area distribution of the galvanic coatings discussed (points in Fig. 3), by using the method of least squares, approximate formulas for the bearing ratio t_p ($t_p = b\epsilon^{\nu}$) were derived, and next its values were computed for the relative separation distance ε, equal 20 %. Results are listed in Table 2. From the list it is clear that copper coating is characterized by the highest bearing ratio (for the given distance)—ca. 10 %, whereas the least bearing ratio is revealed by a chromium coating (ca. 1 %). When we compare the initial situation that is the bearing capacity of the steel disk prior to its coating (ca. 2 %), we must conclude that for majority of analyzed coatings their bearing properties improved significantly with respect to the steel pin, reaching the maximum result (fivefold) in the case of copper. An exception here was the chromium coating in the case of which we observed a drop in the bearing ratio (ca. 50 % in relation to the disk without coatings).

3.3 Measurement of the Coefficient of Friction

The T-01M pin-on-disk testing device was used to measure the coefficient of friction. It is a distributed contact of the plane-to-plane type. With the use of the T-01M testing device the friction coefficients were determined for different metallic coatings (disks) at sliding on steel (pins). The tests were carried out for different surface pressures as a function of the distance covered (friction time) at a given sliding velocity.

Three independent series of friction force measurement (tribological tests) were conducted for each material combination and a given surface pressure/load. Thus the coefficient of friction was determined as a function of the friction path. Final results of the measurements were the arithmetic mean. Both disks and pins were earlier selected for the experiment in such a way that for each measurement series they were characterized by similar roughness profiles (the same class of roughness).

Figure 5 demonstrates the principle of the used tribological tester operation. The examined friction pair consists of a disk rotating with the rotational speed n and a pin pressed to the disk with force P at a point distant by R from the rotation centre of the disk. The pressure is constant throughout the test. Figure 6 shows a picture of a complete station of the pin-on-disk tester T-01M. On the basis of the obtained

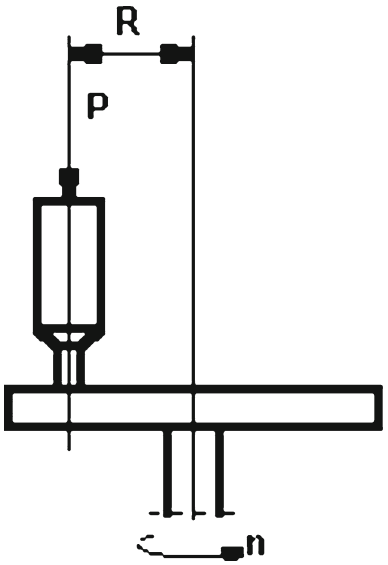

Fig. 5 Schematic diagram of the pin-on-disk tester (T-01M)

Fig. 6 T-01M testing device

tribological characteristics for different frictional pairs the averaged friction coefficients were computed at 120-s intervals. Table 3 presents the averaged results of friction coefficients for three independent measurement series. The experiment was carried out for three different surface pressures: 0.4, 0.8 and 1.2 MPa at a sliding velocity of 0.1 m/s. Such an

Table 3 Mean values of the coefficient of friction for disks with different galvanic coatings for different surface pressures in the first 120 s of the tribological test

Coating	0.4 (MPa)	0.8 (MPa)	1.2 (MPa)
Ni	0.84 ± 0.08	0.90 ± 0.09	0.91 ± 0.09
Cr	0.38 ± 0.04	0.40 ± 0.04	0.43 ± 0.04
Zn	0.42 ± 0.04	0.42 ± 0.04	0.49 ± 0.05
Ag	0.22 ± 0.02	0.21 ± 0.02	0.21 ± 0.02
Cu	0.25 ± 0.03	0.25 ± 0.03	0.26 ± 0.03

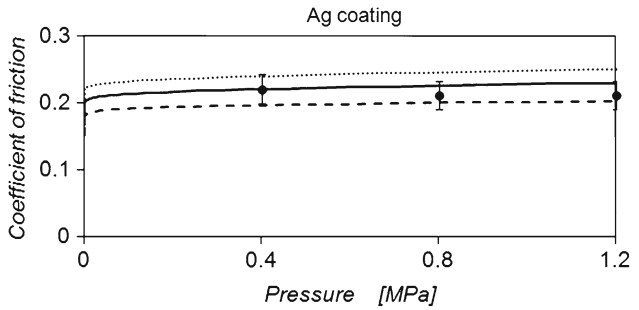

Fig. 7 The friction coefficient as a function of pressure for the steel Ag coating combination for different values of *f*. The top line (*dotted*) corresponds to $f = 0.7$, middle line (*continuous*) corresponds to $f = 0.65$, bottom line (*dashed*) corresponds to $f = 0.6$

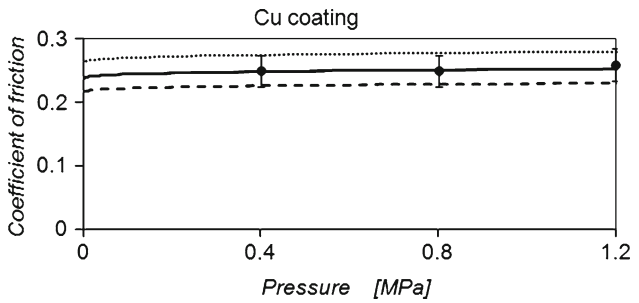

Fig. 8 The friction coefficient as a function of pressure for the steel Cu coating combination for different values of *f* parameter. Top line (*dotted*) corresponds to $f = 0.85$, middle line (*continuous*) corresponds to $f = 0.8$, bottom line (*dashed*) corresponds to $f = 0.75$

approach ensures that roughness parameters measured before the experiment do not change during such a short time.

3.4 Results and Discussion of the Computer Simulation Results for the Coefficient of Friction

Figures 7, 8, 9, 10, 11 present results of the conducted computer simulation of the coefficient of friction depending on the pressure per unit area with the use of data included in Table 1. The Figures presented below also comprise the averaged experimental data for the friction coefficients from the initial 120 s of the run together with determined errors.

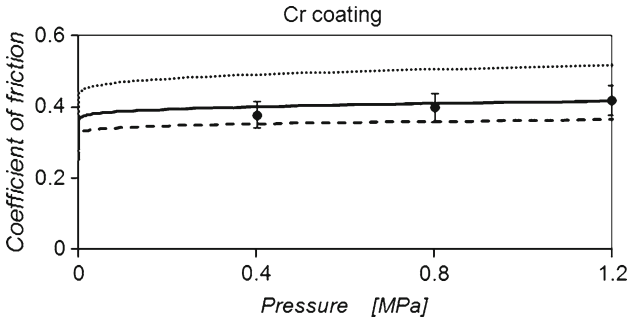

Fig. 9 The friction coefficient as a function of pressure for the steel Cr coating for different values of the *f* parameter. Top line (*dotted*) corresponds to $f = 0.95$, middle line (*continuous*) corresponds to $f = 0.9$, bottom line (*dashed*) corresponds to $f = 0.85$

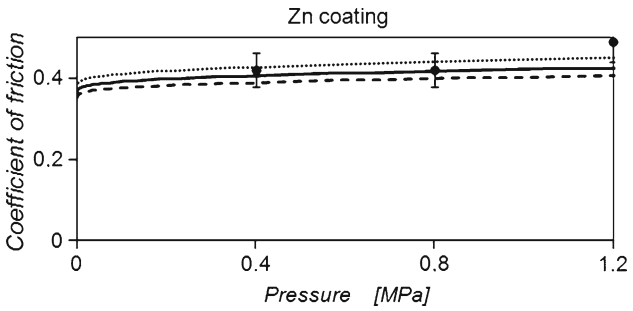

Fig. 10 The friction coefficient as a function of pressure for the steel Zn coating for different values of the *f* parameter. Top line (*dotted*) corresponds to $f = 0.96$, middle line (*continuous*) corresponds to $f = 0.95$, bottom line (*dashed*) corresponds to $f = 0.94$

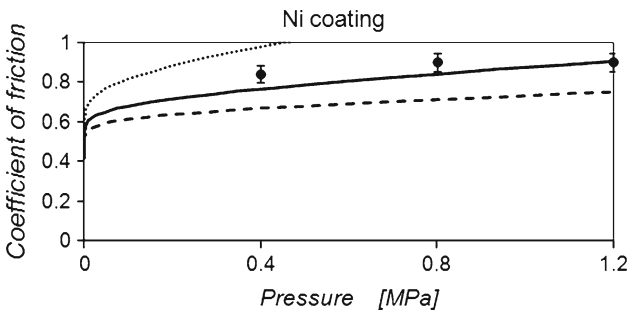

Fig. 11 The friction coefficient as a function of pressure for the steel Ni coating combination for different values of the *f* parameter. Top line (*dotted*) corresponds to $f = 0.997$, middle line (*continuous*) corresponds to $f = 0.996$, bottom line (*dashed*) corresponds to $f = 0.995$

The relationships presented in Figs. 7, 8, 9, 10, 11 were computed for several values of the *f* parameter (relative molecular resistance). The values were selected in such a way as to obtain the best match with experimental results. Data analysis proves that the interaction between silver and steel is the poorest ($f = 0.65 \pm 0.05$), whereas for nickel it is the strongest ($f = 0.996 \pm 0.001$). After we have grouped the obtained values of the relative molecular resistance "f" in the ascending order, we can also order the following series of ele-

ments: silver ($f = 0.65 \pm 0.05$), copper ($f = 0.80 \pm 0.05$), chromium ($f = 0.90 \pm 0.05$), zinc ($f = 0.95 \pm 0.01$), nickel ($f = 0.99 \pm 0.01$), whose adhesive interactions with steel should also increase respectively. In summary it must be emphasized that theoretical results concerning coefficient f are characterized by high compliance both qualitative and quantitative with experimental tests conducted by Rabinowicz [50]. Their ascending values coincide with the tendency to create increasingly more durable adhesive connections with the metals examined. It is an indirect confirmation of the adopted model. In the discussed theoretical model gradation of the f parameter defining adhesive interactions and not its concrete values is important.

4 Conclusions

The paper presents a new mathematical model describing interactions of two rough surfaces which takes into account a plastic interaction described by the theory of the slip-line. It clearly differs from that published by Oxley and his followers because it takes into account a spatial contact of the asperity as well as a statistical distribution of asperity heights. For the sake of calculations it uses basic parameters characterizing these asperities such as: the curvature radius, maximum height and their surface density as well as material constants. It allows us to determine the normal and friction forces and the friction coefficient. In the case of works based on the Oxley model, the authors analyze the contact of a single asperity with a plane and in this way they conclude about the macroscopic coefficient of friction.

The formulas describing the forces of friction and pressure are presented in the form of integral parametric equations set by means of triple integrals. They are connected by a global parameter of surface distance d defining mutual overlapping of the highest asperities. These equations can be solved numerically only. Due to the occurrence of trigonometric and exponential functions the model is characterized by a high computational complexity.

In order to verify theoretical considerations, experimental tests were carried out in the system consisting of a steel disk with a galvanic coating and a steel pin.

One of the elements necessary to carry out a computer simulation is the knowledge of asperity height distributions. These functions were determined on the basis of experimental measurements of bearing curves for individual samples. Analysis of the bearing ratio shows that for the examined samples a Gaussian distribution can describe asperity height distributions. During a comparison with a steel sample it was found out that the process of a thin coating deposition does not change the type of the asperity height distribution, but it modifies parameters characterizing it, for instance the values of standard deviation and the mean value.

The conducted tribological tests resulted in a number of interesting results which are conformable with the solutions reached via a computer simulation. Among the different galvanic coatings tested, the nickel coating was characterized by the highest resistance to motion, whereas the silver one revealed the lowest resistance to motion. The resistance in question results mainly from adhesive interactions, characterized by the f parameter, of the contacting surfaces accompanying plastic interactions. The f coefficient is comprised in the range from 0.65 to values close to 1 and it can be sequenced as follows:

$$f(\mathrm{Ag}) < f(\mathrm{Cu}) < f(\mathrm{Cr}) < f(\mathrm{Zn}) < f(\mathrm{Ni}).$$

Changes in the coefficient of friction as a function of time and pressure are increasing and they can approximately be sequenced as below:

$$\mu(\mathrm{Ag}) < \mu(\mathrm{Cu}) < \mu(\mathrm{Zn}) < \mu(\mathrm{Cr}) < \mu(\mathrm{Ni}).$$

On the basis of the experimental results obtained and conducted computer simulations we can conclude that in the area of plastic interactions and within the range of adopted loads the proposed model of friction predicts resistance to motion correctly.

Acknowledgments The authors wish to thank the reviewers for their very constructive and helpful comments which are important to improve the manuscript.

References

1. Greenwood, J.A.; Williamson, J.B.P.: Contact of nominally flat surfaces. Proc. R. Soc. A. **295**, 300–319 (1966)
2. Adams, G.; Nosonovsky, M.: Contact modeling—Forces. Tribol. Int. **33**, 431–442 (2000)
3. Bhushan, B.: Contact mechanics of rough surfaces in tribology: multiple asperity contacts. Tribol. Lett. **4**, 1–35 (1998)
4. Liu, G.; Wang, Q.; Lin, C.: A survey of current models for simulating the contact between rough surface. Tribol. Trans. **42**, 581–591 (1999)
5. Barber, J.; Ciavarella, M.: Contact mechanics. Int. J. Solids Struct. **37**, 29–43 (2000)
6. Buczkowski, R.; Kleiber, M.: Statistical models of rough surfaces for finite element 3D-contact. Anal. Arch. Comput. Methods Eng. **16**, 399–424 (2009)
7. Greenwood, J.A.; Tripp, J.H.: The contact of two nominally flat rough surfaces. Proc. Inst. Mech. Eng. **185**, 625–633 (1970)
8. Jedynak, R.; Gilewicz, J.: Approximation of smooth functions by weighted means of N-point Pade approximants. Ukr. Math. J. **65**(10), 1410–1419 (2013)
9. Whitehouse, D.J.; Archard, J.F.: The properties of random surfaces of significance in their contact. Proc. R. Soc. Lond. A. **316**, 97–121 (1970)

10. Nayak, P.R.: Random process model of rough surfaces. AMSE J. Lubr. Technol. **93**, 398–407 (1971)
11. Hisakado, T.; Tsukizoe, T.: Effects of distribution of surface slopes and flow pressures of contact asperities on contact between solid surfaces. Wear **30**, 213–227 (1974)
12. Bush, A.; Gibson, R.; Thomas, T.: The elastic contact of rough surfaces. Wear **5**, 87–111 (1975)
13. Bush, A.W.; Gibson, R.D.; Keogh, G.P.: Strongly anisotropic rough surfaces. ASME J. Lubr. Technol. **101**, 15–20 (1979)
14. McCool, J.I.: Relating profile instrument measurements to the functional performance of rough surfaces. ASME J. Tribol. **109**, 264–270 (1987)
15. McCool, J.I.: Extending the capability of the Greenwood Williamson microcontact model. J. Tribol. **122**, 496–502 (2000)
16. Chang W.R.; Etsion I.; Bogy D.B.: Elastic plastic model for the contact of rough surfaces. ASME J. Tribol. **109**, 257–262 (1987)
17. Zhao Y.; Maletta D.M.; Chang L.: An asperity microcontact model incorporating the transition from elastic deformation to fully plastic flow. ASME J. Tribol. **122**, 86–93 (2000)
18. Persson B.N.J.: Contact mechanics for randomly rough surfaces. Surf. Sci. Rep. **61**, 201–227 (2006)
19. Majumdar, A.; Bhushan, B.: Fractal model of elastic–plastic contact between rough surfaces. ASME J. Tribol. **113**, 1–11 (1991)
20. Jackson, R.L.; Streator, J.L.: A multi-scale model for contact between rough surfaces. Wear **261**, 1337–1347 (2006)
21. Jackson, R.L.: An analytical solution to an Archard-type fractal rough surface contact model. Tribol. Trans. **53**, 543–553 (2010)
22. Ciavarella, M.; Delfine, V.; Demelio, G.: A "re-vitalized" Greenwood and Williamson model of elastic contact between fractal surfaces. J. Mech. Phys. Solids. **54**, 2569–2591 (2006)
23. Ciavarella, M.; Greenwood, J.A.; Paggi, M.: Inclusion of "interaction" in the Greenwood and Williamson contact theory. Wear **265**, 729–734 (2008)
24. Whitehouse, D.J.: Fractal or fiction. Wear **249**, 345–353 (2001)
25. Greenwood, J.A.: Comments on 'Fractal or fiction' by DJ Whitehouse. Wear **252**, 842–843 (2002)
26. Kogut, L.; Etsion, I.: Elastic–plastic contact analysis of a sphere and a rigid flat. J. Appl. Mech. Trans. ASME **69**, 657–662 (2002)
27. Jackson, R.; Duvvuru, R.; Menghani, H.; Mahajan, M.: An analysis of elasto-plastic sliding spherical asperity interaction. Wear **262**, 210–219 (2007)
28. Malayamurthi, R.; Marappan, R.: Elastic plastic contact behavior of a sphere loaded against a rigid flat. Mech. Adv. Mater. Struct. (15), 364–370 (2008)
29. Shankar, S.; Mayuram, M.M.: Sliding interaction and wear studies between two hemispherical asperities based on finite element approach. Int. J. Surf. Sci. Eng. **2**, 71–83 (2008)
30. Vijaywargiya, R.; Green, I.: A finite element study of the deformations, forces, stress formations, and energy losses in sliding cylindrical contacts. Int. J. Non Linear Mech. **42**, 914–927 (2007)
31. Mulvihill, D.M.; Kartal, M.E.; Nowell, D.; Hills D.A.: An elastic–plastic asperity interaction model for sliding friction. Tribol. Int. **44**, 1679–1694 (2011)
32. Kogut, L.; Etsion, I.: A finite element based elastic–plastic model for the contact of rough surfaces. Tribol. Trans. **46**, 383–390 (2003)
33. Cohen, D.; Kligerman Y.; Etsion I.: A model for contact and static friction of nominally flat rough surfaces under full stick contact condition. J. Tribol. **130**, 031401–9 (2008)
34. Abdo, J.: Finite element analysis of rough surfaces based on ultimate stress asperity concept. Surf. Interface Anal. **40**, 858–862 (2008)
35. Jackson, R.L.; Green, I.: On the modeling of elastic contact between rough surfaces. Tribol. Trans. **54**, 300–314 (2011)
36. Pawar, G.; Pawlus, P.; Etsion, I.; Raeymaekers, B.: The effect of determining topography parameters on analyzing elastic contact between isotropic rough surfaces. J. Tribol. Trans. ASME **135**, 011401–10 (2013)
37. Robbe-Valloire, F.: Statistical analysis of asperities on a rough surface. Wear **249**, 401–408 (2001)
38. Kapłonek, W.; Nadolny, K.: The diagnostics of abrasive tools after internal cylindrical grinding of hard-to-cut materials by means of a laser technique using imaging and analysis of scattered light. Arab. J. Sci. Eng. **38**, 953–970 (2013)
39. Abdo, J.: Experimental technique to study tangential-to-normal contact load ratio. Tribol. Trans. 48, 389–403(2005)
40. Sepehri, A.; Farhang, K.: A finite element-based elastic–plastic model for the contact of rough surfaces. Model. Simul. Eng. (2011). doi:10.1155/2011/561828
41. Karpenko, Y.A.; Akay A.: A numerical model of friction between rough surfaces. Tribol. Int. **34**, 531–545 (2001)
42. Shcheglovov, A.; Schavelin, V.: Thermal conductivity of the elastic contact roughness surfaces in a vacuum. J. Frict. Wear **7**, 91–98 (1986)
43. Kopalinsky, E.; Oxley P.: An investigation of sliding metallic wear in the presence of thin film boundary lubrication. Tribol. Interface Eng. **38**, 629–637 (2000)
44. Jamari, J.; Schipper, D.: Experimental investigation of fully plastic contact of a sphere against a hard flat. ASME J. Tribol. **128**, 230–235 (2006)
45. Bressana, J.; Williams, J.: Mathematical slip-line field solutions for ploughing a hard particle over a softer material. Wear **267**, 1865–1872 (2009)
46. Jahanandish, M.; Veiskarami, M.; Ghahramani, A.: Effect of foundation size and roughness on the bearing capacity factor, Ng, by stress level-based ZEL method. Arab. J. Sci. Eng. **37**, 1817–1831
47. Whitehouse, D.: Handbook of surface metrology. Institute of physics Publishing, Bristol Philadelphia (1994)
48. Nediu, B.; Jovanoviu, D.: Influence of previous machining on characteristics of galvanic coatings. In: SERBIATRIB '11 12th International Conference on Tribology, pp. 146–151 (2011)
49. Sulek, W.; Jedynak, R.: Frictional forming of electroplated copper and zinc coatings. Int. J. Appl. Mech. Eng. **7**, 183–187 (2002)
50. Rabinowicz, E.: Friction and wear of materials. Wiley-Interscience, USA (1995)